Available online at www.sciencedirect.com
ScienceDirect
Quaternary Research 68 (2007) 387–399
QUATERNARY RESEARCH
www.elsevier.com/locate/yqres

Cirque glacier activity in arctic Norway during the last deglaciation

Øyvind Paasche [a,b,*], Svein Olaf Dahl [c,b], Jostein Bakke [b], Reidar Løvlie [a], Atle Nesje [a,b]

[a] Department of Earth Science, University of Bergen, Allégt. 41, N-5007 Bergen, Norway
[b] Bjerknes Centre for Climate Research, Allégt. 55, N-5007, Bergen, Norway
[c] Department of Geography, University of Bergen Fosswinkelsgt. 6, N-5020, Bergen, Norway

Received 21 September 2006
Available online 21 September 2007

Abstract

Numerous cirques of the Lofoten–Vesterålen archipelago in northern Norway have distinct moraine sequences that previously have been assigned to the Allerød-Younger Dryas (~13,400 to 11,700 yr BP) interval, constraining the regional distribution of the equilibrium-line altitude (ELA) of cirque and valley glaciers. Here we present evidence from a once glacier-fed lake on southern Andøya that contests this view. Analyses of radiocarbon dated lacustrine sediments including rock magnetic parameters, grain size, organic matter, dry bulk density and visual interpretation suggest that no glacier was present in the low-lying cirque during the Younger Dryas-Allerød. The initiation of the glacial retreat commenced with the onset of the Bølling warming (~14,700 yr BP) and was completed by the onset of Allerød Interstade (~13,400 yr BP). The reconstructed glacier stages of the investigated cirque coincide with a cool and dry period from ~17,500 to 14,700 yr BP and a somewhat larger Last Glacial Maximum (LGM) advance possibly occurring between ~21,050 and 19,100 yr BP.

Keywords: Seasonality; Younger Dryas; Norway; Glacier; ELA

Introduction

The cooling of the North Atlantic region during the Younger Dryas (12,800–11,670 yr BP) have traditionally been attributed to a reduction of the Atlantic meridional overturning circulation (AMOC) (Broecker et al., 1985), but considerable uncertainty remains to the scope of this weakening (Jansen, 1987; McManus et al., 2004), and also the manner in which it influenced the Northern Hemisphere climate (Seager and Battisti, 2007). The Scandinavian mainland experienced large-scale climate changes not only during the Younger Dryas, but also at the onset of the Bølling warming (14,700 yr BP). Producing reliable reconstructions of late glacial climate (defined here as the period between 14,700 and 11,670 yr BP) in order to better understand the impact of this variability has proven difficult because the Fennoscandian Ice Sheet (FIS) still covered much of the continental areas (e.g., Mangerud, 2004) at this time. Nevertheless, sustained efforts have secured valuable paleoclimatic information from several coastal sites in Norway (e.g., Birks et al., 2005 and references therein), which shed light on the late glacial transition in this area.

State-of-the-art pollen and macrofossil-based temperature reconstructions obtained from various lakes along the Norwegian coast from 58°N to 72°N show a fairly uniform summer cooling during the Younger Dryas of some 4 °C (e.g., Birks et al., 2005), which suggests that the difference between north and south summer temperature was about the same as the modern one. In contrast, winter temperatures were lowered 6–7 °C in the south and ~12 °C in the north (Birks et al., 2005), indicating that the wintertime difference between north and south had increased ~5 °C. Regardless of the forcing mechanisms responsible for the Younger Dryas cooling, this suggests that cooling was more efficient in the north than in the south during the winter, and that summer temperatures remained essentially unchanged. When compared to the Bølling–Allerød interval it becomes evident that the summer temperature difference between the two periods was minor (~1 °C) in both the south and the north, but that the

* Corresponding author. Bjerknes Centre for Climate Research, Norway. Fax: +47 55 589803.
E-mail address: Oyvind.paasche@bjerknes.uib.no (Ø. Paasche).

0033-5894/$ - see front matter © 2007 University of Washington. All rights reserved.
doi:10.1016/j.yqres.2007.07.006

difference in winter temperatures was greater (Birks et al., 2005). It appears therefore that the greatest climate variability (i.e. temperature) during the entire late glacial was confined to the winter season.

The purpose of this paper is to investigate the seasonal climatic impact of the Younger Dryas cooling and the preceding interstadial in northern Norway by reconstructing cirque glacier activity. Both the summer and the winter season can be evaluated from such records. The site chosen for this task is a cirque valley located on Andøya, the northernmost island in the Lofoten–Vesterålen complex, containing a lake that once received meltwater from a small upstream glacier. This research exploits the various qualities of the glacio-lacustrine sediments retrieved from the once glacier-fed lake, in combination with geomorphological mapping. We compare glacier-based evidence with paleoclimatic reconstructions from other terrestrial sites in the North Atlantic as well as with marine data from the Nordic Seas.

Although the combination of glacial geomorphology and coring of downstream lakes in glacierized catchments can produce unique information about past glacier activity (Karlén, 1976, 1981; Nesje et al., 1991; Matthews and Karlén, 1992; Dahl and Nesje, 1996), this commonly requires analysis of multiple sedimentary characteristics (Jansson et al., 2005). Clastic sediments that have been eroded and transported within glacierized catchments have been exposed to several interacting processes before they are deposited in downstream lakes. Factors such as source bedrock, glacier size, potential transport length and lake bathymetry should be taken into consideration when making inferences about past glacier activity (Østrem, 1975, 1987; Leonard, 1985, 1986). Unscrambling the minerogenic sediments that are retrieved from glacier-fed lakes (which includes both fluvial and paraglacial contributions; Church and Ryder, 1972; Church and Gilbert, 1975; Weirich, 1985) is necessary if one is to isolate the glacial component. In order to achieve this, a suite of methods has been employed, with particular emphasis on rock magnetic properties and grain-size analyses.

Study site

Lake Nermark (162 m a.s.l.) is located on the southern part of Andøya (Fig. 1), which is the northernmost island (69°N 16°E, 490 km^2) of the Lofoten–Vesterålen archipelago. The lake is situated in the outer rim of a mature cirque valley with a southeastern aspect. An equal-sized lake (Trollvatnet) lies

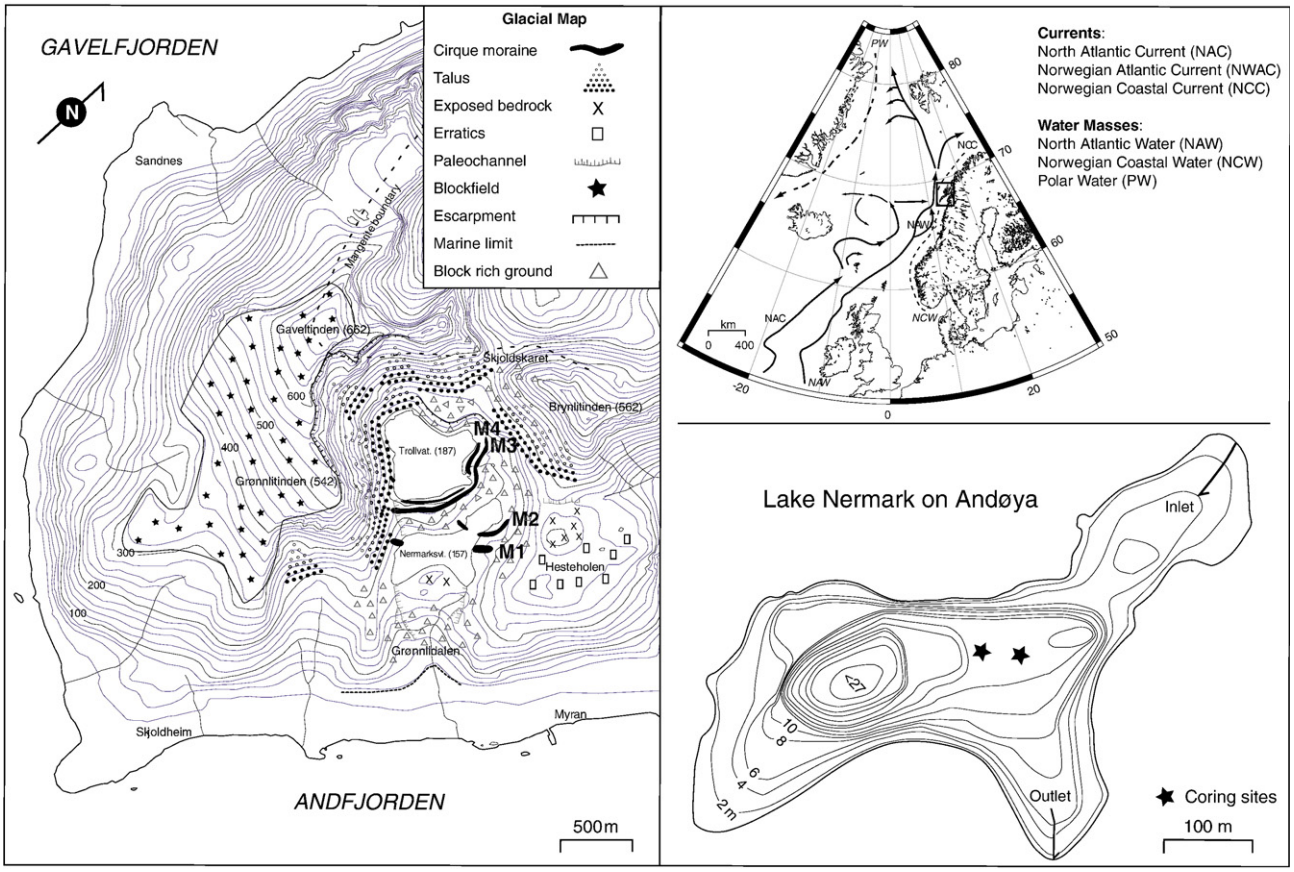

Figure 1. Left panel: Glacial map of southern Andøya showing the distribution of surficial deposits and selected landforms located within the study area. The moraine sequence delineates four former glacier positions labeled as M1, M2, M3 and M4. The mangerite bedrock boundary is shown as a dashed line. Upper right panel: Andøya (490 km^2) is the northernmost island of the Lofoten–Vesterålen archipelago, situated in a highly maritime climate only 20 km from the edge of the continental margin. The study site lies on the southern tip of Andøya within a mature cirque having a southeasterly aspect and hosting two well-defined lakes with bedrock thresholds. Lower right panel: The bathymetry of lake Nermark was measured and mapped by echo sounding. The two stars represent the coring sites.

https://doi.org/10.1016/j.yqres.2007.07.006 Published online by Cambridge University Press

upstream (Fig. 1). The southern part of the watershed is made up of migmatitic gneiss exhibiting irregular quartz intrusions. The gneiss is replaced by a partly porfyric granite that can be traced along the northern shores of both the local lakes, making up a bedrock terrace. This granite merges into a dark mangerite dominating the northern and northwestern mountains in the watershed (Fig. 1). This rock is known to contain magnetite among other minerals (Henningsen and Tveten, 1998).

The present climate is maritime, with mean annual air temperature of 3.8 °C and mean annual precipitation of 1100 mm (Aune, 1993; Førland, 1993). The Norwegian Atlantic current (NWAC) passes just west of Andøya exerts considerable influence on the regional climate, creating anomalously warm conditions for the latitude. The 7.2 Sverdrup ($1Sv = 10^6\ m^3\ S^{-1}$) strong NWAC splits into two northward branches (Fig. 1) leading into the Barents Sea (2.4 Sv) and the Fram Strait (4.8 Sv) (Gascard et al., 2004).

Methods

Mapping and coring

Geomorphological features within the investigated catchment were mapped during 2 weeks of fieldwork complemented with aerial photograph interpretation (scale 1:40,000; Fig. 1). A high-resolution bathymetric map of Lake Nermark was obtained through continuous echo-sounding measurements along 14 transects (Fig. 1). A piston corer (Nesje, 1992) operated from the lake-ice surface was used to retrieve two cores (diameter 11 cm) from Lake Nermark, and the longer core (185 cm) was examined in detail.

Quantitative parameters and chronology

The sediment cores were split and lithological characteristics were visually described (Fig. 2). Loss-on-ignition (LOI), a measurement of the organic matter/organic carbon content (Dean, 1974) and dry-bulk-density (DBD) were measured every half-centimeter ($n = 352$), whereas grain-size analyses were conducted every centimeter (100–184 cm; $n = 84$) using a Sedigraph 5100 (Stein, 1985). Basic rock magnetic parameters such as magnetic susceptibility (χbulk), anhysteretic remanent magnetization (ARM) and saturation isothermal remanent magnetization (SIRM) were determined every centimeter with $2 \times 2 \times 2$ cm samples ($n = 185$).

Five plant macrofossils used for radiocarbon dating were washed, purified with distilled water, dried overnight at 100 °C and stored in airtight glasses before analysis. Two additional bulk samples were dried overnight at 100 °C and put in airtight plastic bags. The Poznan Radiocarbon Laboratory performed the ^{14}C-dating (AMS) and dates were calibrated with CALIB 4.4 (Stuiver et al., 1998). An age-depth model was obtained using a mix-effect weighted regression procedure (Heegaard et al., 2005) (Fig. 2).

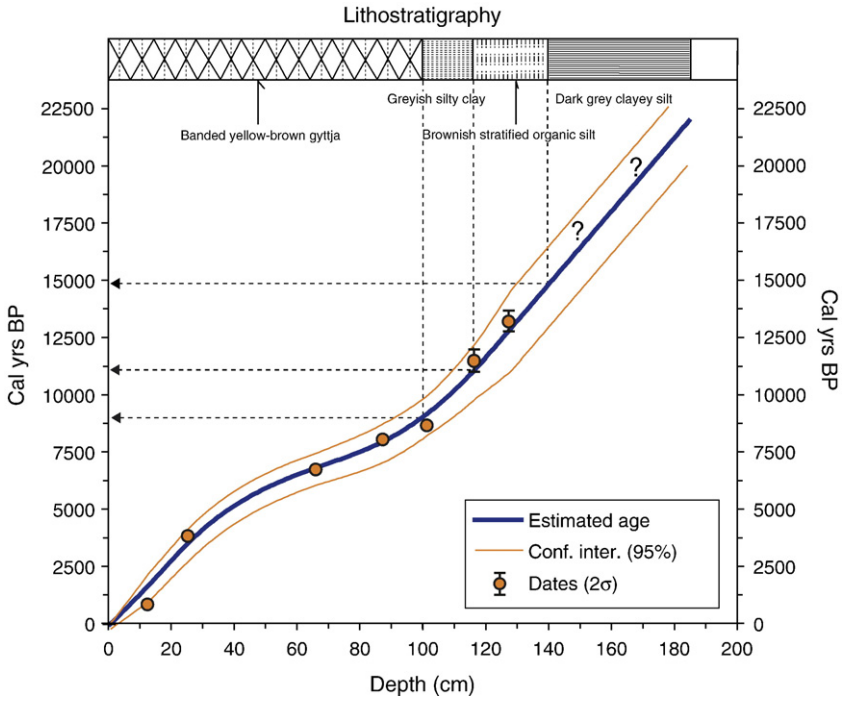

Figure 2. Seven radiocarbon forms the basis of the age-depth model that assumes that the top of the core represent the present. The five youngest ages are obtained on plant macrofossils, whereas the two oldest dates were obtained for bulk sediment samples. No carbon is present in the bedrock of the catchment (Tveten, E., personal communication, 2006) nor is there any evidence for old carbon contamination in other lakes in northern Andøya during the same interval (Vorren et al., 1988). The age-depth modeling was constructed with a mix-effect weighted regression procedure where the individual uncertainties (one standard deviation) of the dates are incorporated into the model (Heegaard et al., 2005). Error bars (2σ) are smaller than the dot representing the calibrated age, except for the oldest two dates. The simplified lithostratigraphy shows four individual sedimentary units partly corresponding to the chronozone boundaries.

https://doi.org/10.1016/j.yqres.2007.07.006 Published online by Cambridge University Press

Glaciers and equilibrium-line altitudes (ELA)

The equilibrium-line altitude (ELA) represents the mean elevation of the boundary that separates accumulation from ablation, and for glaciers in steady state the accumulation–area ratio (AAR) is usually in the vicinity of 0.6 ± 0.05 (Porter, 1970, 1975). Annual mass balance of glaciers at mid to high latitudes is primarily controlled by two meteorological constraints (1) summer temperature (1 May–30 September, the ablation season) and winter precipitation (1 October–30 April, the accumulation season) (e.g., Ahlmann, 1935; Liestøl, 1967). Empirical data collected near the ELA at 10 Norwegian glaciers, located between 60°13′ N and 66°39′ N in climate regimes ranging from being maritime to continental, suggest a strong exponential relationship between these two variables ($A = 0.915e^{0.339T}$, where A is in meters water equivalent and T is in degrees Celsius; henceforth referred to as the Liestøl equation), which implies that winter precipitation (P_w) can be calculated if one knows the summer (T_s) temperature or *vice versa* (Liestøl in Sissons, 1979; Sutherland, 1984; Ballantyne, 1989, 1990; Dahl and Nesje, 1996). Due to their rapid response time, small glaciers can swiftly adjust their geometry and size to compensate for either positive or negative changes of their mass balance, usually manifested by vertical movement of the ELA. Excess leeward accumulation of windblown snow might, however, lower the ELA beyond the aforementioned climatic constraints and its effect should be taken into account (Dahl and Nesje, 1992).

The reconstruction of the glacier configuration presented here was achieved by mapping terminal moraines in addition to applying the AAR method (Porter, 1970). The D/A ratio was invoked in order to correct the ELA for local redistribution of wind-driven snow (see Dahl and Nesje, 1992; Dahl et al., 1997). The drainage area (D) above the former ELA is divided on the accumulation zone (A) of the reconstructed cirque glacier in order to reduce the potential positive effect that wind-driven snow might have on the ELA. The ELA of small temperate cirque glaciers is, however, usually not higher than the highest point found on the associated lateral moraines (e.g., Andrews, 1975), but may be somewhat higher if the glacier is frozen to its bed (Clark et al., 1994).

Results

Mapping

Geomorphic mapping reveals a moraine sequence recording four individual glacier positions (Fig. 1). The limits of the two innermost moraines (M3 and M4) are unambiguous and can be traced continuously between Lake Trollvatnet and Lake Nermark (Fig. 1). The two ridges are closely spaced (<30 m) and occasionally interconnected. Relict meltwater channels are located near the present-day outlet from Lake Trollvatnet and can be traced back to a breach in the northern part of the moraine ridges (Fig. 1). Another subtle relict meltwater channel is present on the southern side of the lake. The outline of the third moraine (M2) delineates a former glacier tongue extending partly into Lake Nermark. Remnants of the fourth and outermost moraine (M1) are located on both sides of the lake and represents what appears to have been the maximum extension of the cirque glacier, though it might have coalesced with a glacier occupying Andfjorden at an earlier time. Erratics located on Hesteholen, the hilltop situated to the northeast of Lake Nermark (Fig. 1), indicates a significantly larger glacier advance than that associated with the fourth moraine described above.

Sedimentary properties

The core lithostratigraphy consists of homogenous dark grey clayey silt (184–140 cm) grading upwards into brownish stratified organic silt (139–116 cm) that is in turn overlain by greyish silty clay (116–100 cm) (Fig. 2). Yellow-brown gyttja with irregularly spaced darker bands from 0.3 to 1 cm thick dominates from 100 cm to the top of the core. The presence of stratified layers in large parts of the core suggests that there has been little or no disturbance due to coring or transport. The age-depth model indicates modest changes in the sedimentation rate throughout the last 13,200 yr BP (Fig. 2). Age estimates beyond the lowest date are an extrapolation of the age-depth model.

The rock magnetic parameterization together with LOI (%) and DBD (g/cm^3) is presented in Figure 3. The magnetic mineralogy, as recorded by the S-ratio ($\sigma IRM_{100mT}/\sigma IRM_{3T}$), indicates magnetite up to ~14 000 yr followed by a sharp shift towards 'harder' or lower values that could be indicative of hematite (Stober and Thompson, 1979). A peak centred at 10,500 yr BP also shows values associated with magnetite, contrary to the fluctuating harder values found in the remaining part of the core. Magnetic susceptibility (χbulk), χARM and σSIRM document similar trends throughout the core, though with greater differences after ~10,000 yr BP. The strong magnetic susceptibility ($\sim 6.5 \times 10^{-7}$ m^3 kg^{-1}) found in the oldest part of the core is punctuated by a brief interval (19,000–17,300 yr BP) of lower values ($\sim 1.4 \times 10^{-7}$ m^3 kg^{-1}) that seems to initiate a continuous weakening of the signal. The stable period from 13,260 to 11,520 yr BP shows an order of magnitude lower values compared to the previous period and is terminated by a brief return towards higher values ($\sim 1.6 \times 10^{-7}$ m^3 kg^{-1}). The described patterns above are reproduced by both χARM and σSIRM. A similar development is also evident from the σARM/σSIRM ratio where a steady fining in magnetic grain size starts just prior to 16,000 yr BP, following a fairly stable period. This trend accelerates from 14,800 yr BP until it resumes a somewhat more stable mode. From 8000 yr BP towards the present the magnetic grain size displays a gradual shift towards finer fractions.

LOI values prior to 13,200 yr BP are typically below 5%, but subsequently the signal is dominated by higher values and stronger variability. A distinct drop back to lower values is reached around 10,450 yr BP. Since LOI and DBD are negatively correlated throughout the core (Fig. 4) the latter parameter follow more-or-less the same pattern as the former, although changes in DBD in the early part of the record is more

https://doi.org/10.1016/j.yqres.2007.07.006 Published online by Cambridge University Press

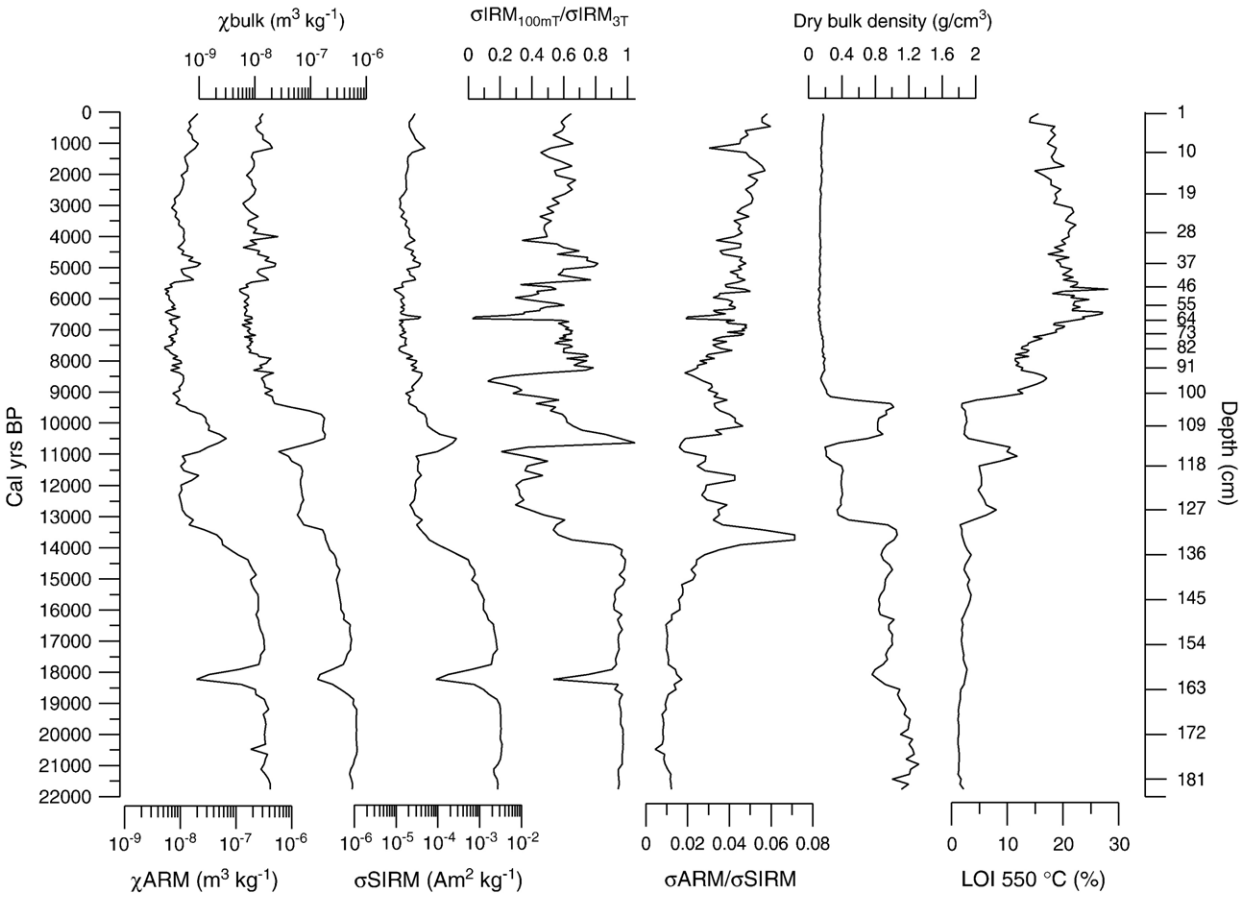

Figure 3. Downcore variations of rock magnetic parameters in addition to bulk density and loss-on-ignition (LOI).

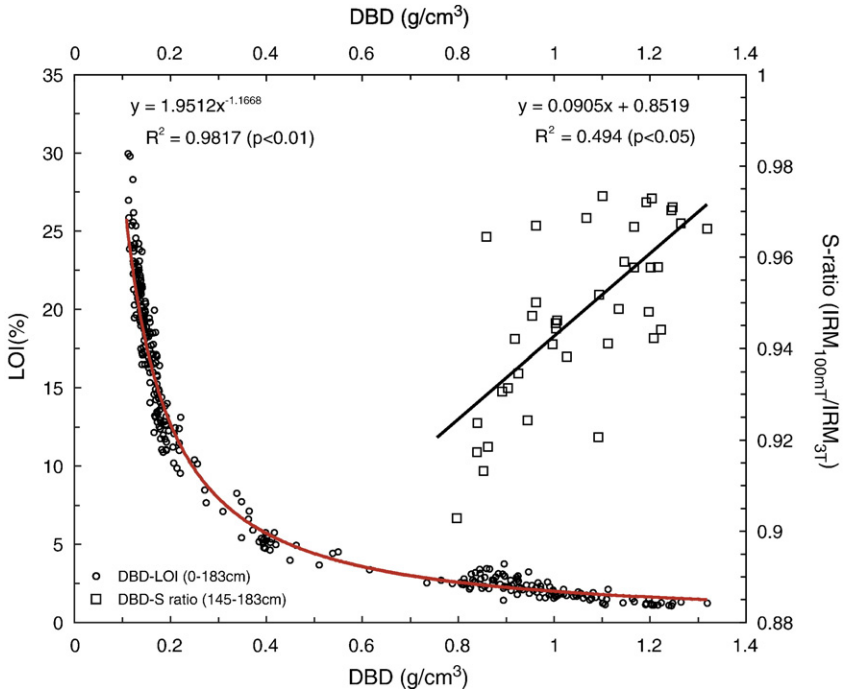

Figure 4. The statistical strength of dry bulk density (DBD) (g/cm^3) against LOI (%) and S-ratio (σIRM100$_{mT}$/σIRM$_{3T}$).

https://doi.org/10.1016/j.yqres.2007.07.006 Published online by Cambridge University Press

pronounced than LOI. Moreover, the highest DBD values (1.2 to 1.3 g/cm^3) in the entire record are found in the oldest part of the core and they do not decrease to lower values until 18,500 yr BP.

Downcore variations in grain size (<64 μm) reveal a polymodal sediment distribution consisting mainly of clay and very fine silt (Fig. 5). Mean (μm) grain size indicates upward fining culminating in a rapid increase around 13,800 yr BP and subsequently a relatively stable period between 13 000 and 9000 yr BP (Fig. 5). Clay (<2 μm) is the dominant fraction making up nearly 50% of the grain-size distribution. However, there is considerable variability within the record. Regression analyses suggest that there is a strong negative relationship between clay and fine silt ($r^2=0.81$ ($p<0.01$), medium silt ($r^2=0.9$ ($p<0.01$)) and coarse silt ($r^2=0.67$ ($p<0.01$)), implying that the clay fraction to some extent is 'controlled' by the combined changes of fine silt (4–8 μm), medium silt (8–16 μm) and coarse silt (16–31 μm). This suggests that as long as the source was the same, changes in grain-size composition were primarily driven by changes in discharge of the river entering Lake Nermark.

Cross correlation of different sedimentary parameters reveal a covariance that might help to explain variations in dry-bulk-density (DBD). The significant positive correlation between DBD versus medium silt and coarse silt indicates that higher dry-bulk-density values are associated with higher influx of grains ranging from 8 to 31 μm in the time before 13,200 yr BP (Fig. 6A). The correlation between DBD and magnetic susceptibility indicates that the physical grain-size range 8–31 μm contains the strongest magnetic signal. From Figure 6B, it is clear that the two parameters covary, but that this pattern is reversed after 14,200 yr BP. The magnetic mineralogy, as indicated by the S-ratio, covaries with the DBD in the period before 10,000 yr BP and hence connects the influx of magnetite versus harder magnetic minerals to the variations of the DBD (Fig. 4).

ELA reconstructions

The topography of the cirque and the position of the terminal moraines indicates that the glacier shape, and particularly its hypsometry, were relatively simple, which otherwise might be a source of error when using the AAR relationship (Furbish and Andrews, 1984). With an accumulation–area ratio of 0.6±0.05, the reconstructed glacier (~0.78 km^2) has a mean ELA of 268±16 m during the deposition of the two innermost moraines, M3 and M4 (Fig. 7). The close spacing of these moraines implies that the difference in ELA is minor and beyond the resolution of the AAR method. Similarly, the reconstructed ELA of the glacier during deposition of moraine M1 and M2 is 247±17 m (~1.1 km^2).

A statistical–empirical model of glacier ELAs (Lie et al., 2003) is utilized here in conjunction with the previously described 'Liestøl equation' to estimate the theoretical modern ELA at southern Andøya to be c. 1500 m a.s.l. The model of Lie et al. (2003) has successfully been used to investigate glacier-climate

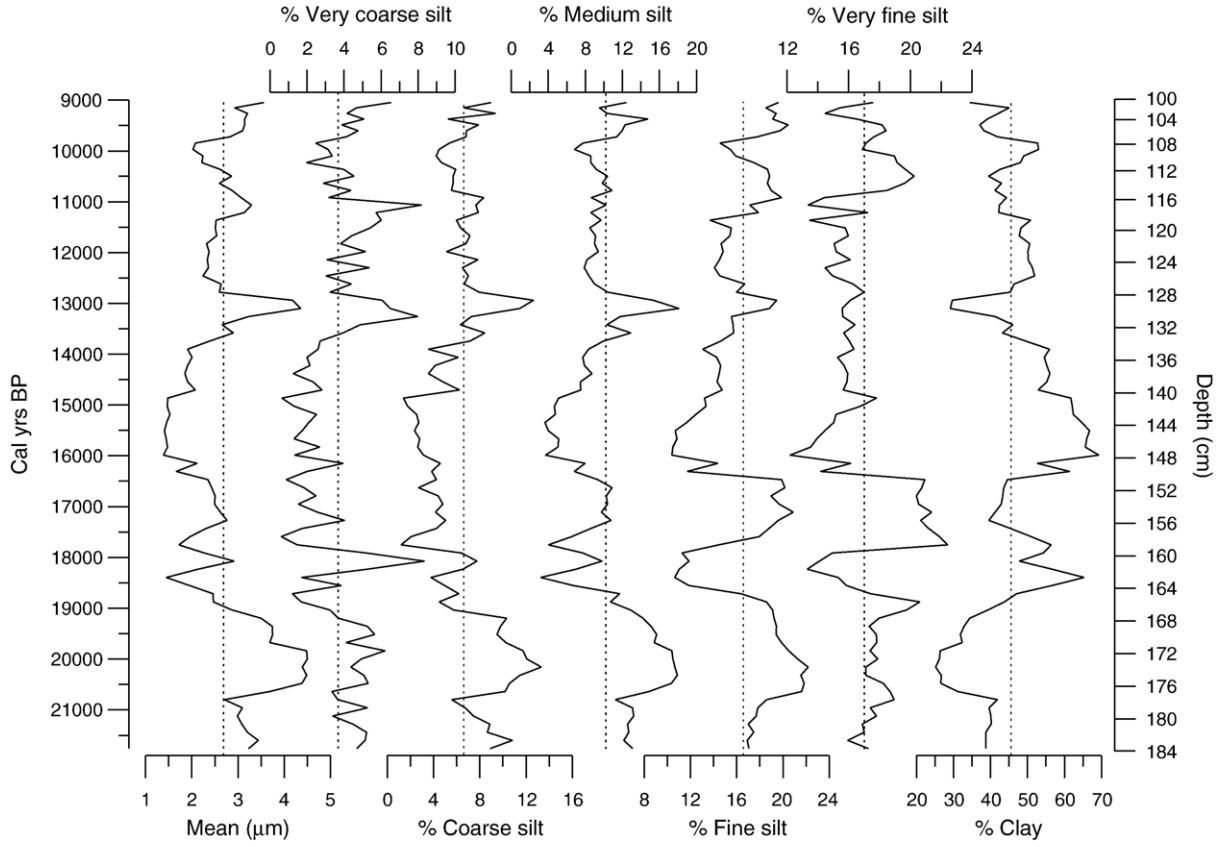

Figure 5. Grain-size distribution for the interval between 100–184 cm depth. The dotted line represents the arithmetic mean of the individual classes.

https://doi.org/10.1016/j.yqres.2007.07.006 Published online by Cambridge University Press

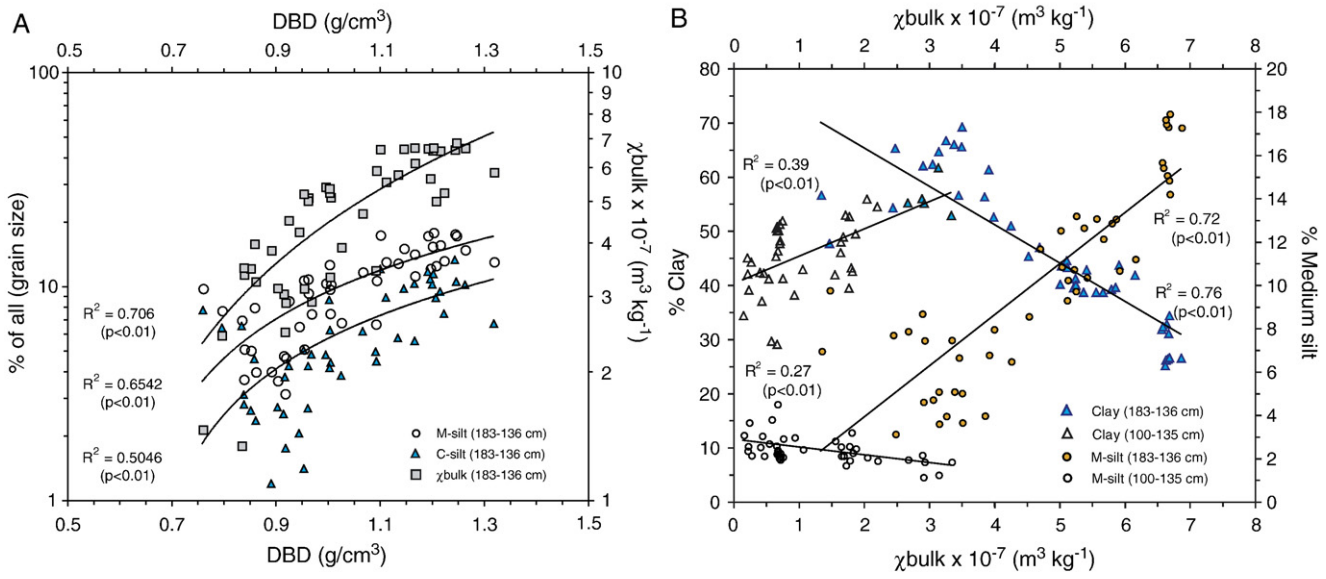

Figure 6. (A) The statistical strength of dry bulk density (g/cm^3) against medium silt (%), coarse silt (%) and χbulk (m^3 kg^{-1}). (B) The regressions between χbulk (m^3 kg^{-1}) versus clay (%) and medium silt (%), disclosing that above 135 cm the relationship is reversed. The solid lines are best-fit curves.

relationships in Greenland, USA, Scandinavia and the European Alps on different temporal scales (Kovanen and Slaymaker, 2005; Rasmussen and Conway, 2005; Steiner et al., 2005; Ivy-Ochs et al., 2006; Lie and Paasche, 2006; Zemp et al., 2007).

Considering an ELA of ~270 m during the youngest cirque glaciation stage (M3 and M4), the depression of the theoretical ELA would be 1230 m, which corresponds to a 7.4 °C cooling using an environmental lapse rate of 0.6 °C/100 m. In comparison, the ELA estimate of the oldest cirque glaciation stage (M1 and M2) of ~250 m would require a cooling of 7.5 °C. As illustrated in Figure 7 there are no great changes in the configuration of the paleo ice-bodies during the different advances, except for a down-glacier ice mass displacement. No land-uplift adjustments were taken into consideration since the Younger Dryas sea level were within that of the present-day ±2 m (Fjalstad, 1997).

Possible glacier scenarios and winter precipitation estimates

Pollen-based reconstructions from northern Andøya, shown in Figure 8, indicate mean July air temperatures (T_J) of 7 °C during the Younger Dryas (Alm, 1993), which is in agreement with reconstructions from sites farther north that also indicate mean July temperatures of 6–7 °C (Fimreite et al., 2002; Birks et

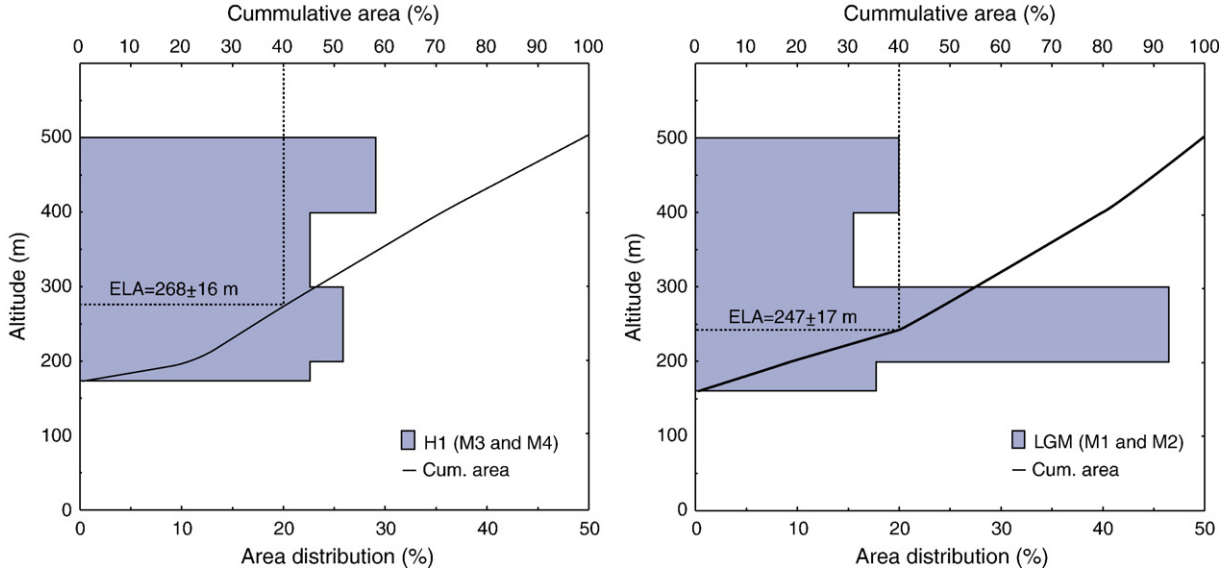

Figure 7. Area–altitude distribution of the former glaciers occupying the cirque located on southern Andøya during deposition of moraines M1–M2 (LGM scenario) and moraines M3–M4 (H1 scenario). The age of H1 ranges from 17,500 to 14,700 yr BP (Hemming, 2004), whereas a possible age for LGM is ~19,100 to 21,050 yr BP. The estimated ELA of the individual glacier stages was achieved by applying an AAR of 0.6±0.05.

https://doi.org/10.1016/j.yqres.2007.07.006 Published online by Cambridge University Press

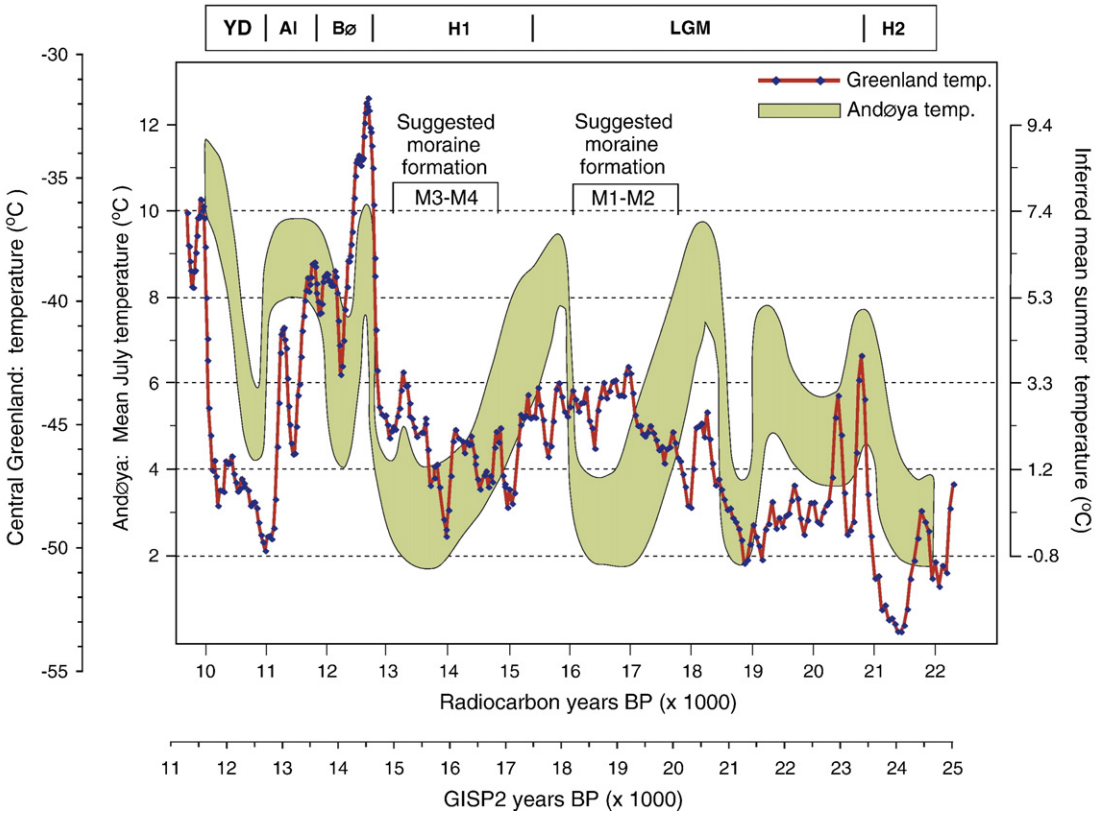

Figure 8. Reconstructed mean July temperature (thick curve) on Andøya (Alm, 1993) as compared with reconstructed temperature at central Greenland (thin curve) for the period encompassing the last deglaciation (Alley, 2000). The *y*-axis on the right side shows the inferred mean summer temperature on Andøya, which was obtained by applying the using the regression equation presented in Figure 9B. Note the discrepancy between the two temperature records for the time between 17,700 and 14,500 yr BP, commonly known as H1, which might be related to the large sea ice extent at this time. The two innermost moraines (M3–M4), as previously presented in Figure 1, are suggested to have been deposited during the H1, whereas the somewhat larger advances (M1–M2) might be related to the equally cold and dry period lasting from ~19,100 to 21,050 yr BP.

al., 2005). A Younger Dryas climate scenario for the cirque glacier may therefore be evaluated since T_J and the ELA are known, but first we must convert T_J into T_s because that is what the Liestøl equation requires. Using the $T_s - T_J$ conversion regression shown in Figure. 9B and correcting for altitude, the estimated T_s at an ELA of ~270 m is 2.2 °C. With T_s of 2.2 °C the Liestøl equation predicts a winter precipitation (P_w) of 1990 mm (or 925 mm with the D/A ratio of 2.15), which is more than twice the modern value (Fig. 9A). Taking account for possible uncertainties associated with the temperature reconstruction of 7 °C, and the ELA estimate for the glacier while depositing moraines M3 and M4, these results does not support the presence of cirque glacier during the Younger Dryas unless winter precipitation was much higher than modern values. Calculating the temperature depression associated with the difference between the present-day ELA and the ELA during deposition of moraines M3 and M4, which necessarily represents the youngest advance, can further test the Younger Dryas scenario.

The difference between the theoretical ELA above southern Andøya (~1500 m) and the estimated ELA for the glacier (~270 m) during deposition of moraines M3 and M4 is 1230 m, which equals a T_s cooling of 7.4 °C. With a present-day T_s of 7.3 °C it suggests that the T_s at an ELA of 270 m may have been in the vicinity of −0.1 °C, or a T_J of 2.7 °C if the $T_s - T_J$ regression equation is applied (Fig. 9B). This is twice as cold as the reconstructed temperatures were during the Younger Dryas, so it seems that the Younger Dryas scenario can be ruled out, but there are earlier periods that corresponds to T_J of 2.7 °C, namely the 'High Arctic' period encompassing ~17,500 to 14,760 yr BP on Andøya, with T_J fluctuating around 3 °C (see Fig. 8)–a interval also known as Henrich Event 1 (H1) (Hemming et al., 2004). With T_s of −0.1 °C the 'Liestøl equation' suggests, after correcting for a D/A ratio of 2.5, a winter precipitation of 426 mm, which seems reasonable.

The negligible difference between the ELAs during deposition of moraines (M1–M2 and M3–M4) suggests that the climatic constrains were of similar magnitude. We therefore assume that the deposition of moraines M1 and M2 occurred during an equally cold phase as H1, the most likely candidate is the LGM period lasting from ~21,050–19,100 yr BP (Fig. 8). Because the D/A ratio number (1.48) is lower than for the H1 scenario (Fig. 7) it might indicate somewhat more humid winter conditions during LGM.

Discussion

Late glacial sedimentary characteristics

Several significant sedimentary changes occurred in Lake Nermark around 14,000 yr BP that can be related to corres-

https://doi.org/10.1016/j.yqres.2007.07.006 Published online by Cambridge University Press

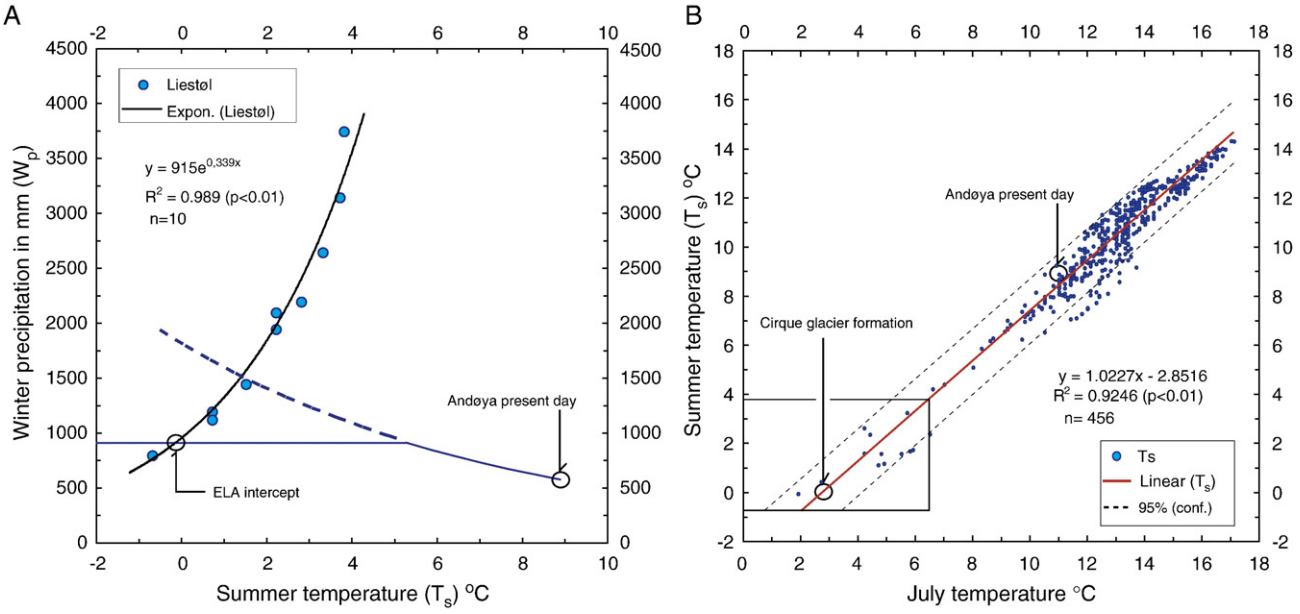

Figure 9. (A) The 'Liestøl equation' based on measurements made on the 10 Norwegian glaciers is shown together with the climate adjustment required for suppressing the ELA sufficient to ensure glacier formation (black line). If winter precipitation is allowed to increase into the free atmosphere the intercept with the Liestøl relationship is somewhat higher, than if it is tied up to the highest altitude of the surrounding mountain (dashed line). (B) The statistical strength between summer temperature (May–September) and July temperature based on 456 Norwegian metrological stations (1961–1990) (Aune, 1993). The inserted square represents the climatic range of the glaciers on which Olav Liestøl made the original measurements.

ponding adjustments in erosion and transport of material within the catchment. The disappearance of magnetite at this time, as inferred from the S-ratio, suggests a changing source for the clastic material deposited in Lake Nermark. This unequivocal shift towards magnetically 'harder' values is also registered as a decrease in the DBD values (Fig. 3). An increase in organic matter commencing at ~13,200 yr BP reflects a reduced influx of minerogenic material, which is also in accordance with lower DBD values. The concentration-dependent rock magnetic parameters χARM and σSIRM also show a steady weakening of the signal towards 14,000 yr BP, whereupon the values decline more rapidly. The magnetic susceptibility (χbulk) signal follows the same pattern as χARM and σSIRM, although somewhat lagged, as the signal remains high until 13,400 yr BP.

The source for the 'soft' S-ratios is most likely the magnetite-bearing mangerite located in the northwestern part of the watershed. The agent responsible for eroding the mangerite and transporting the material must have ceased to exist concurrent with the change in the magnetic mineralogy around ~14,000 yr BP. The steady decline in the concentration-dependent parameters indicates, however, that this transition may not have been instantaneous.

The slow demise of a small cirque glacier was most likely responsible for the observed sedimentary shift during the late glacial. The retreat of the glacier would explain the sudden absence of magnetite as it would no longer erode into the mangerite and subsequently transport the material down to the adjacent lake where the bulk would be trapped. The inferred size of the glacier (~0.78 km^2) at the onset of retreat was most likely connected to the two innermost moraine ridges (M3 and M4), even though the actual deposition of the moraines must obviously have occurred sometime before the retreat started.

There are no observations to indicate that any of the clastic sediment studied here relates to the cirque glacier when it was large enough to reach down to Lake Nermark and deposit moraine M2. At this time the coring site would have been less than 200 m from the glacier snout and deposition would have been affected by the proximity of the glacier in terms of grain size and sediment composition, as discussed below.

Glacier conditions inferred from lake sediments

A positive empirical relationship between meltwater discharge and sediment transport has been documented in glacierized catchments (e.g., Østrem, 1975). The capacity of glacial streams to transport sediment in suspension and through bedload movement is determined by the general interdependency of water velocity, grain size and density (Hjulström, 1939; Sundborg, 1956, 1967). A depositional interface occurs when streams enter lakes where the majority of the transferred sediments are trapped, even though some of the finer material can escape in open-ended systems (Østrem, 1975). The average grain size of suspended sediments settling in glacier-fed lakes is often smaller than 63 μm according to empirical data (Weirich, 1985; Leemann and Niessen, 1994; Matthews et al., 2000; Lie et al., 2004; Bakke et al., 2005a,b). The coarser material is commonly deposited close to the inlet/delta of the lake, whereas deposition of the finer sediments (<31 μm) increases with distance from river inlet (Hatling, 1967). When the ratio of the glacier area versus catchment area is low, the run-off will be strongly affected by melting (i.e. summer temperature) and

https://doi.org/10.1016/j.yqres.2007.07.006 Published online by Cambridge University Press

hence highest during the summer months (e.g., Church and Gilbert, 1975). This is particularly the case for polythermal glaciers located within permafrost regimes, considering the brief summer season (June-August) and the few potential aquifers besides the glacier (e.g., Woo, 1986; Hodgkins et al., 2003).

The grain-size analyses from Lake Nermark show high clay content suggesting that the glacial meltwater discharge and the overall sediment yield were very low during the glacial phase (Fig. 5). The short distance between the glacier terminus and Lake Nermark reduces the potential for intermediate sediment storage reservoirs that otherwise could represent a source for sudden changes in the grain-size distribution. Investigations of proglacial lakes receiving sediments primarily from polythermal glaciers located on Svalbard (Svendsen et al., 1987; Mäusbacher et al., 2002) and in southern Norway (e.g., Lie et al., 2004) all show remarkable high clay contents (~20–50%), even though higher proportions of coarser material is associated with enhanced glacier activity (Matthews et al., 2000; Lie et al., 2004). The difference in specific sediment yields between polythermal and temperate glaciers has also been shown to be considerable (Hallet et al., 1996; Bogen and Bønsnes, 2003). This is partly due to the fact that the ablation area of polythermal glaciers is usually frozen to the substratum (e.g., Paterson, 1994), restricting erosion as well as meltwater access to important sediment reservoirs, and hence causing reduced sediment availability (Gurnell, 1987). Even so, it has been shown that cold-based glaciers can entrain basal sediments at a reduced scale (Cuffey et al., 2000). Hodson et al. (1998) have also emphasized the importance of adjoining moraine systems and other downstream surficial deposits as sources and sinks for suspended sediments transported by glacial meltwater streams.

It seems reasonable to assume that the glacier responsible for the sedimentary flux into Lake Nermark basically was polythermal, with a cold-based ablation zone that restricted the composition (mostly fine grained sediments), amount and the magnitude of transported clastic material. The demise of this small glacier occurred without any catastrophic events and was most likely initiated by the onset of the Bølling warming some 14,700 yr BP, which means that the innermost moraines (M3 and M4) were formed some time before. The reconstructed summer temperature (T_s) of −0.1 °C and winter precipitation (P_w) of 426 mm derived from the required ELA lowering associated with the deposition of moraines M3 and M4 (the H1 scenario) is in good agreement with a polythermal glacier (cf. Paterson, 1994). Given the moraine sequence present in the cirque (Fig. 1), then the two outermost ridges (M1 and M2) must represent an older age, but the climate was probably similar to that reconstructed for the H1 scenario. A reasonable age for the glacier advance associated with M1 and M2 is the LGM scenario, when the climate was similar to that of H1.

There is no evidence for a rejuvenation of any glacier beyond the final deglaciation, but the brief clastic phase that follows immediately after the onset of the Holocene suggests a landscape adjustment that could have been related to permafrost subsidence (cf. Paasche et al., 2007).

The ELA estimates and the impact of wind

The plateau southwest of the cirque (Fig. 1) represents a potential source for windblown snow that could provide additional accumulation, in particular if the prevailing wind direction was towards north-northeast. It is difficult to assess this effect for a number of reasons (e.g., Kuhle, 1988), including uncertainties regarding the direction of the wind field during the accumulation season and potential precipitation gradients (Humlum, 2002). Even so, Dahl et al. (1997) suggest that the effect of wind can (and should) be taken into account by means of the D/A ratio. It should be stressed that the D/A relationship only offers a rough estimate of the potential wind effect on the ELA distribution, but other studies have shown how important snow drifting can to cirque glaciation (Humlum, 1997). The ratio numbers for the two assessed ELAs presented in Figure 7 is 2.15 (H1) and 1.48 (LGM), indicating that the contribution from windblown snow might have had a certain influence. This is in accordance with summer temperature estimates derived from the Liestølen equation (see Fig. 9A), which show that the winter precipitation must have been higher than today for the ELA to be lowered sufficiently to enable cirque glacier formation during the Younger Dryas. A significantly increase in winter precipitation during the Younger Dryas is contrary to that reported by paleodata. Alley (2000) records a 70% reduction in winter precipitation at the time on Greenland, whereas Bakke et al. (2005a,b) observe a 40% in northern Norway. Model simulations also shows significantly less winter precipitation in northern Scandinavia during the Younger Dryas (Renssen et al., 2001), suggesting that wetter conditions were highly unlikely.

Regional climate implications

The concept that most moraines in the Lofoten–Vesterålen complex were deposited during the Younger Dryas and the Allerød (Rasmussen, 1984; Andersen, 1968) is not supported by the results presented here. The cirque glacier reconstruction from Andøya shows that the ELA was not low enough for glaciers to form below 600 m for this time interval. As elegantly demonstrated by the Liestøl equation (Fig. 9A), relatively warm summer temperatures need to be counterbalanced by wet winters if the ELA are to be sustained; that was apparently not the case on Andøya or possibly in the rest of Lofoten and Vesterålen during the late glacial. Other cirque glaciers in northern Norway that survived the Bølling warming might have experienced only modest advances during the Younger Dryas, as was the case for cirque and valley glaciers at Svalbard due to an effective precipitation starvation (Mangerud and Landvik, 2007).

The enhanced seasonality difference along the Norwegian coast during the late glacial (Birks et al., 2005) was constrained to the winter season, causing northern Norway to be progressively colder than the south. The explanation for this geographically skewed seasonality could be related to rapid adjustments of the sea-ice, which would cut off the moisture supply, reducing the potential amount of winter precipitation.

https://doi.org/10.1016/j.yqres.2007.07.006 Published online by Cambridge University Press

The maximum southern sea-ice margin during the Younger Dryas in the Nordic Seas has yet to be accurately reconstructed, although several works indicate that it was located south of Andøya (69°N) (e.g., Koc et al., 1993) and even down to the British Isles (Denton et al., 2005). The fact that a pronounced seasonality difference did exist along the Norwegian coast during the late glacial indicates perhaps that the sea-ice extension did not advance beyond southwestern Norway (cf. Lie and Paasche, 2006). Moreover, if sea-ice was the primary force modulating the seasonality difference between the summer and the winter season in the North Atlantic sector during the Younger Dryas, it might also be reasonable to expect that the observed difference in temperature were matched by abrupt regional shifts in the precipitation pattern.

Quantitative summer temperature reconstructions from Andøya show that there is a similar development for northern Norway (Alm, 1993) and central Greenland (Alley, 2000) during the late glacial (Fig. 8), but that significant difference exists in the period before. The warming event that precedes H1 (17,500–14,700 yr BP) (e.g., Hemming, 2004), and also a cooling around 18,500 yr BP, are not recorded in GISP2 (Fig. 8). In contrast, variability in the AMOC, as seen from the $^{231}Pa/^{230}Th$ ratio (McManus et al., 2004), is very similar to the July temperature reconstruction from Andøya (Fig. 8), showing a near complete shutdown during H1 when July temperature remained very cold (3 °C), but also a much stronger circulation just prior to H1 corresponding to a warming on Andøya. The sea-ice probably extended farther south during H1 than during the Younger Dryas causing an extremely arid and cool climate in the North Atlantic region, and possibly with a less pronounced seasonality difference that we observe for the late glacial.

The glacier reconstructions presented here shows that the climate conditions on Andøya during H1 and LGM, with ELAs between 270 and 250 m, was similar in terms of summer temperature (T_s), with values around 0.1 °C, and a corresponding winter precipitation (P_w) of 420 mm or so. This suggests perhaps that other similar cirques located in the Lofoten–Vesterålen archipelago also contains paleoenvironmental information extending all the way back to the LGM, and that larger areas of the Archipelago was ice-free than previously assumed (cf. Rasmussen, 1984).

Conclusions

Evidence for a previously unrecognized cirque glacier advance during the last deglaciation has been established for southern Andøya through lake coring of a once glacier-fed lake, in combination with geomorphological mapping of the surrounding watershed. Rock magnetic parameters, grain-size analyses and complementing physical properties of the lacustrine sediments within a partly radiocarbon constrained age-depth model have enabled construction of a continuous paleoclimatic record.

The moraine sequence in the cirque has revealed four glacier stages that advanced beyond Trollvatnet, of which two reached into Lake Nermark. The reconstructed glacier hypsometry of former glaciers indicates a balanced area distribution between the accumulation and ablation zones. The equilibrium-line altitudes of the four different glacial stages (M1, M2, M3 and M4) lie within ±30 m. The largest glacier (1.1 km^2) had an ELA of 247±17 m compared to the smallest glacier (0.78 km^2) with an ELA of 268±16 m. The depression of the theoretical ELA during these periods was estimated to be in the order of ~1230 m.

Sedimentary characteristics indicate that only glaciofluvial deposits corresponding to the most restricted glacier stage (M3 andM4) have been recorded in the investigated core. The final recession of the smallest and youngest glacier started with the onset of the Bølling warm spell 14,700 yr BP, and by the beginning of the Allerød Interstade (~13,400 yr BP) the glacier had melted completely. No glacier rejuvenated after this complete retreat.

Using the 'Liestøl equation' in combination with the AAR method, a possible climatic scenario allowing for glacier formation on southern Andøya suggests a summer temperature colder than −0.1 °C, which equals to a T_s lowering of ~7.4 °C compared to the present-day climate. The period ranging from 17,500 to 14,700 yr BP (H1) meet these climatic requirements, according to the temperature reconstruction provided from northern Andøya (Alm, 1993). The corresponding winter precipitation estimate for the H1 period was just above 400 mm.

Climate conditions during the formation of the largest glacier advance (M1 and M2) were similar to those occurring during H1, with cool arctic summers and dry winters. Accepting a continuous moraine chronology the outermost moraines must be older than H1 and may have been formed during a cool period spanning from ~21,050 to 19,100 yr BP. The lower D/A relationship during this period indicates somewhat more humid conditions than during the H1.

The results of this work fail to support the presence of local glaciers during both Allerød and Younger Dryas, implying regional ELA higher than 600 m along the western coast of Vesterålen. This is in stark contrast to earlier studies, which assumed that the majority of the cirque moraines located in the Lofoten–Vesterålen region formed during the Allerød-Younger Dryas chronozones (e.g., Rasmussen, 1984). An ELA depression of only 380 m during the Younger Dryas (Bakke et al., 2005a) would leave large areas of Lofoten–Vesterålen unglacierized, supporting our results. The climatic reason for this restricted depression was probably the combination of relatively warm summer and dry winters, where the latter were driven by an annual expansion of sea-ice extending south of Lofoten–Vesterålen.

Acknowledgments

ØP are grateful to Bjørn Kvisvik and Jørund Strømsøe for excellent field assistance and Einar Heegaard for constructing the age-depth model. Dr. Ann Hirt provided valuable comments on the use of rock magnetic parameters, as did Prof. Ole Humlum on the glacier reconstruction. ØP wants to thank Dr. Øyvind Lie for stimulating discussions concerning the use of ELAs in a paleo context. ØP would also like to acknowledge the

important feedback given by Prof. Ed Evanson, Prof. Jeffrey S, Munroe, two anonymous reviewers and editor-in-chief Prof. Eric Steig. This work has been supported by NORPEC, an NFR funded Strategic program headed by Prof. H.J.B. Birks. This is publication Nr. A 163 for the Bjerknes Centre for Climate Research.

References

Ahlmann, H.W., 1935. The Fourtheenth of July Glacier. Geografiska Annaler 17, 167–218.

Alley, R.B., 2000. The Younger Dryas cold interval as viewed from central Greenland. Quaternary Science Reviews 19, 213–226.

Alm, T., 1993. Øvre Æråsvatn—Palynostratigraphy of a 22,000 to 10,000 BP lacustrine record on Andøya, northern Norway. Boreas 22, 171–188.

Andersen, B.G., 1968. Glacial Geology of Northern Nordland, North Norway. Norwegian Geological Survey 320, 1–74.

Andrews, J.T., 1975. Glacial Systems—An Approach to Glaciers and Their Environments. Duxberry Press, Massachusetts. 199 pp.

Aune, B., 1993. Air temperature normal, 1961–1990. The Norwegian Meteorological Institute. Report 2.

Bakke, J., Dahl, S.O., Paasche, Ø., Løvlie, R., Nesje, A., 2005a. Glacier fluctuations, equilibrium-line altitudes and palaeoclimate in Lyngen, northern Norway, during the Lateglacial and Holocene. The Holocene 15, 518–540.

Bakke, J., Lie, Ø., Nesje, A., Dahl, S.O., Paasche, Ø., 2005b. Utilizing physical sediment variability in glacier-fed lakes for continuous glacier reconstructions during the Holocene, northern Folgefonna, western Norway. The Holocene 15, 161–176.

Ballantyne, C.K., 1989. The Loch Lomond Advance on the Isle of Skye, Scotland: glacier reconstruction and palaeoclimatic implications. Journal of Quaternary Science 4, 95–108.

Ballantyne, C.K., 1990. The Holocene glacial history of Lyngshalvøya, northern Norway: chronology and climatic implications. Boreas 19, 93–117.

Birks, H.H., Kiltgaard Kristensen, D.K., Dokken, T.M., Andersson, C., 2005. Explanatory comparisons of quantitative temperature estimates over the last deglaciation in Norway and the Norwegian Sea. In: Drange, H., Dokken, T.M., Furevik, T., Gerdes, R., Berger, W. (Eds.), The Nordic Seas; An Integrated Perspective; Oceanography, Climatology, Biogeochemistry, and Modeling. Geophysical Monograph, vol. 158. AGU, Washington, DC, pp. 341–355.

Bogen, J., Bønsnes, T.E., 2003. Erosion and sediment transport in High Arctic rivers, Svalbard. Polar Research 22, 175–189.

Broecker, W.S., Peteet, D., Rind, D., 1985. Does the ocean–atmosphere system have more than one mode? Nature 315, 21–25.

Church, M., Gilbert, R., 1975. Proglacial fluvial and lacustrine environments. In: Joupling, A.V., McDonald, B.C. (Eds.), Glaciofluvial and Glaciolacustrine Sedimentation, vol. 23. SEPM Special Publication, pp. 22–100.

Church, M., Ryder, J.M., 1972. Paraglacial sedimentation: a consideration of fluvial processes conditioned by glaciation. Geological Society of America Bulletin 83, 3059–3072.

Clark, D.H., Clark, M.M., Gillespie, A.R., 1994. Debris-covered glaciers in Sierra-Nevada, California, and their implications for snowline reconstructions. Quaternary Research 41, 139–153.

Cuffey, K., Conway, H., Gades, A.M., Hallet, B., Lorrain, R., Severinghaus, J.P., Steig, E.J., Vaughn, B., White, J.W.C., 2000. Entrainment at cold glacier beds. Geology 28, 351–354.

Dahl, S.O., Nesje, A., 1992. Paleoclimatic implications based on equilibrium-line altitude depressions of reconstructed Younger Dryas and Holocene cirque glaciers in inner Nordfjord, western Norway. Palaeogeography, Palaeoclimatology, Palaeoecology 94, 87–97.

Dahl, S.O., Nesje, A., 1996. A new approach to calculating Holocene winter precipitation by combining glacier equilibrium-line altitudes and pine-tree limits: a case study from Hardangerjøkulen, central southern Norway. The Holocene 6, 381–398.

Dahl, S.O., Nesje, A., Øvstedal, J., 1997. Cirque glaciers as morphological evidence for a thin Younger Dryas ice sheet in east-central Southern Norway. Boreas 26, 161–180.

Dean, W.E., 1974. Determination of carbonate and organic matter in calcareous sediments and sedimentary rocks by rocks by loss on ignition: comparison with other methods. Journal of Sedimentary Petrology 44, 242–248.

Denton, G.H., Alley, R.B., Comer, G.C., Broecker, W.S., 2005. The role of seasonality in abrupt climate change. Quaternary Science Reviews 24, 1159–1182.

Fimreite, S., Vorren, K.-D., Vorren, T., 2002. Vegetation, climate and ice-front oscillations in the Tromsø area, northern Norway during the Allerød and Younger Dryas. Boreas 30, 89–100.

Fjalstad, A. 1997. Late Weichselian glacial maximum, glacial retreat, and postglacial sea level changes at northern and central Andøya, northern Norway. PhD thesis, University of Tromsø.

Furbish, D.J., Andrews, J.T., 1984. The use of Hypsometry to indicate long-term stability and response of valley glaciers to changes in mass transfer. Journal of Glaciology 30, 199–211.

Førland, J., 1993. Precipitation Normal (1961–1990), The Norwegian Meteorological Institute, Report 39.

Gascard, J.C., Raisbeck, G., Sequeira, S., Yiou, F., Mork, K.A., 2004. The Norwegian Atlantic Current in the Lofoten basin inferred from hydrological and tracer data (^{129}I) and its interaction with the Norwegian Coastal Current. Geophysical Research Letters 31, L01308. doi:10.1029/2003GL/018303.

Gurnell, A.M., 1987. Suspended sediment. In: Gurnell, A.M., Clarke, M.J. (Eds.), Glacio-fluvial Sediment Transfer. John Wiley and Sons Ltd., pp. 305–354.

Hallet, B., Hunter, L., Bogen, J., 1996. Rates of erosion and sediment evacuation by glaciers: a review of field data and their implications. Global and Planetary Change 12, 213–235.

Hatling, J. 1967. Slamtransport og geomorfologi i Leirdølas nedslagsfelt (in Norwegian). Unpublished Cand. Scient. Thesis, Department of Geography. University of Oslo, Norway.

Heegaard, E., Birks, H.J.B., Telford, R.J., 2005. Relationships between calibrated ages and depth in stratigraphical sequences: an estimation procedure by mixed-effect regression. The Holocene 15, 612–618.

Hemming, S.R., 2004. Heinrich events: massive Late Pleistocene detritus layers of the North Atlantic and their global climatic imprint. Reviews of Geophysics 42, RG1005. doi:10.1029/2003RG000128.

Henningsen, T., Tveten, E., 1998. Geologisk kart over Norge. Berggrunnskart Andøya, M 1:250 000. Norwegian Geological Survey.

Hjulström, F., 1939. Transportation of detritus by moving water. In: Trask, P.D. (Ed.), Recent Marine Sediments. American Association of Petroleum Geologists, Tulsa, pp. 5–31.

Hodgkins, R., Cooper, R., Wadham, J., Tranter, M., 2003. Suspended sediment fluxes in a high-Arctic glacierised catchment: implications for fluvial storage. Sedimentary Geology 162, 105–117.

Hodson, A.J., Gurnell, A., Tranter, M., Bogen, J., Hagen, J.O., Clark, M., 1998. Suspended sediment yield and transfer processes in a small High-Arctic glacier basin, Svalbard. Hydrological Processes 12, 73–86.

Humlum, O., 1997. Younger Dryas glaciation in Söderåsen, south Sweden: an analysis of meteorological and topographical controls. Geografiska Annaler 79, 1–15.

Humlum, O., 2002. Modelling late 20th-century precipitation in Nordenskiöld Land, Svalbard, by geomorphic means. Norsk Geografisk Tidsskrift 56, 96–103.

Ivy-Ochs, S., Kerschner, H., Kubik, P.W., Schluchter, C., 2006. Glacier response in the European Alps to Heinrich Event 1 cooling: the Gschnitz stadial. Journal of Quaternary Science 21, 115–130.

Jansen, E., 1987. Rapid changes in the inflow of Atlantic water into the Norwegian Sea at the end of the last glaciation. In: Berger, W.H., Labeyrie, L.D. (Eds.), Abrupt Climatic Change. D. Reidel, Dordrecth, pp. 299–310.

Jansson, P., Rosquist, G., Schneider, T., 2005. Glacier fluctuations, suspended sediment flux and glacio-lacustrine sediments. Geografiska Annaler 87, 37–50.

Karlén, W., 1976. Lacustrine sediments and tree-limit variations as indicators of Holocene climatic fluctuations in Lapland, northern Sweden. Geografiska Annaler 58A, 1–34.

Karlén, W., 1981. Lacustrine sediment studies. Geografiska Annaler 63A, 273–281.
Koc, N., Jansen, E., Haflidason, H., 1993. Paleoceanographic reconstructions of surface ocean conditions in the Greenland, Iceland and Norwegian Seas through the last 14-ka based on diatoms. Quaternary Science Reviews 12, 115–140.
Kovanen, D.J., Slaymaker, O., 2005. Fluctuations of the Deming Glacier and theoretical equilibrium line altitudes during the Late Pleistocene and Early Holocene on Mount Baker, Washington, USA. Boreas 34, 157–175.
Kuhle, M., 1988. Topography as the fundamental element of glacial systems. GeoJournal 17, 545–568.
Leemann, A., Niessen, F., 1994. Varv formation and the climatic record in an Alpine proglacial lake: calibrating annually laminated sediments against hydrological and meteorological data. The Holcoene 4, 1–8.
Leonard, E., 1985. Glaciological and climatic controls on lake sedimentation, Canadian Rocky Mountains. Zeitschrift für Gletscherkunde und Glazialgeologie 21, 35–42.
Leonard, E., 1986. Use of lacustrine sedimentary sequences as indicators of holocene glacial history, Banff National Park, Alberta, Canada. Quaternary Research 26, 218–231.
Lie, Ø., Paasche, Ø., 2006. How extreme was northern hemisphere seasonality during the Younger Dryas? Quaternary Science Reviews 25, 404–407.
Lie, Ø., Dahl, S.O., Nesje, A., 2003. A theoretical approach to glacier equilibrium-line altitudes using meteorological data and glacier mass-balance records from southern Norway. The Holocene 13, 365–372.
Lie, Ø., Dahl, S.O., Nesje, A., Matthews, J.A., Sandvold, S., 2004. Holocene fluctuations of a polythermal glacier in high-alpine eastern joutunheimen, central-southern Norway. Quaternary Science Reviews 23, 1925–1945.
Liestøl, O., 1967. Storbreen glacier in Joutunheimen, Norway. Norsk Polarinstitutt, Skrifter 141, 1–63.
Mangerud, J., 2004. Ice sheet limits on Norway and the Norwegian continental shelf. In: Ehlers, J., Gibbard, P. (Eds.), Quaternary Glaciations—Extent and Chronology, vol. 1. Europe Elsevier, Amsterdam, pp. 271–294.
Mangerud, J., Landvik, J.Y., 2007. Younger Dryas cirque glaciers in western Spitsbergen: smaller than during the Little Ice Age. Boreas 36, 278–285.
Matthews, J.A., Karlén, W., 1992. Asynchronous neoglaciation and Holocene climatic change reconstructed from Norwegian glaciolacustrine sedimentary sequences. Geology 20, 991–994.
Matthews, J.A., Dahl, S.O., Nesje, A., Berrisford, M.S., Andersson, C., 2000. Holocene glacier variations in central Jotunheimen, southern Norway based on distal glaciolacustrine sediment cores. Quaternary Science Reviews 19, 1625–1647.
Mäusbacher, R., Borg, K.v.d., Daut, G., Kroemer, E., Müller, J., Wallner, J., 2002. Late Pleistocene and Holocene environmental changes in NW Spitsbergen—Evidence from lake sediments. Zeitschrift für Geomorphologie 46, 417–439.
McManus, J., Francois, R., Gherardi, J.M., Keigwin, L.D., Brown-Leger, S., 2004. Collapse and rapid resumption of Atlantic meridional circulation linked to deglacial climate changes. Nature 428, 834–837.
Nesje, A., 1992. A piston corer for lacustrine and marine sediments. Arctic and Alpine Research 24, 257–259.
Nesje, A., Kvamme, M., Rye, N., Løvlie, R., 1991. Holocene glacial and climatic history of the Jostedalsbreen region, western Norway: evidence from lake sediments and terrestrial deposits. Quaternary Science Reviews 10, 87–114.
Østrem, G., 1975. Sediment transport in glacial meltwater streams. In: Joupling, A.V., McDonald, B.C. (Eds.), Glaciofluvial and Glaciolacustrine Sedimentation, vol. 23. SEPM Special Publication, pp. 101–122.
Østrem, G., Olsen, H.C., 1987. Sedimentation in glacier lake. Geografiska Annaler 69A, 123–138.
Paasche, Ø., Dahl, S.O., Løvlie, R., Bakke, J., Nesje, A., 2007. Rockglacier activity during the Last Glacial–Interglacial transition and Holocene spring snowmelting. Quaternary Science Reviews 26, 793–807.
Paterson, W.S.B., 1994. The Physics of Glaciers, 3rd ed. Pergamon, Oxford.
Porter, S.C., 1970. Quaternary glacial record in Swat Kohistan, West Pakistan. Geological Society of American Bulletin 7, 1421–1446.
Porter, S.C., 1975. Equilibrium-line altitudes of late quaternary glaciers in the Southern Alps, New Zealand. Quaternary Research 5, 27–47.
Rasmussen, A., 1984. Late Weichselian moraine chronology of the Vesterålen islands, North Norway. Norsk Geologisk Tidsskrift 64, 193–219.
Rasmussen, L.A., Conway, H., 2005. Influence of upper-air conditions on glaciers in Scandinavia. Annals of Glaciology 42, 402–408.
Renssen, H., Isarin, R.F.B., Jacob, D., Podzun, R., Vandenberghe, J., 2001. Simulation of the Younger Dryas climate in Europe using a regional climate model nested in an AGCM: preliminary results. Global and Planetary Change 30, 41–57.
Seager, R., Battisti, D.S., 2007. Challenges to our understanding of the general circulation: abrupt climate change. In: Schneider, T., Sobel, A. (Eds.), The General Circulation of the Atmosphere. Princeton University Press, Princeton and Oxford, p. 400.
Sissons, J.B., 1979. Palaeoclimatic inferences from former glaciers in Scotland and the Lake District. Nature 278, 518–521.
Stein, R., 1985. Rapid grain-size analysis of clay and silt fraction by SediGraph 5000D: comparison with Coulter Counter and Atterberg methods. Journal of Sedimentary Petrology 55, 590–593.
Steiner, D., Walter, A., Zumbuhl, H.J., 2005. The application of a non-linear back-propagation neural network to study the mass balance of Grosse Aletschgletscher, Switzerland. Journal of Glaciology 51, 313–323.
Stober, J.C., Thompson, R., 1979. Magnetic remanence acquisition in Finnish lake sediments. Geophysical Journal of the Royal Astronomical Society 57, 727–739.
Stuiver, M., Reimer, P.J., Bard, E., Beck, J.W., Burr, G.S., Hughen, K.A., Kromer, B., McCormac, F.G., v.d. Plicht, J., Spurk, M., 1998. IntCal 98 Radiocarbon Age Calibration, 24000-0 cal BP. Radiocarbon 40, 1041–1083.
Sundborg, A., 1956. The River Klarälven: a study of fluvial processes. Geografiska Annaler 38, 127–316.
Sundborg, A., 1967. Some aspects on fluvial sediments and fluvial morphology. I. General views and graphic methods. Geografiska Annaler 49A, 333–343.
Sutherland, D.G., 1984. Modern glacier characteristics as a basis for inferring former climates with particular reference to the Lomond Stadial. Quaternary Science Reviews 3, 291–309.
Svendsen, J.I., Landvik, J.Y., Mangerud, J., Miller, G.H., 1987. Postglacial marine and lacustrine sediments in Lake Linnévatnet, Svalbard. Polar Research 5, 281–283.
Vorren, T.O., Vorren, K.-D., Alm, T., Gulliksen, S., Løvlie, R., 1988. The last deglaciation (20.000 to 11.000 BP.) on Andøya, northern Norway. Boreas 17, 41–77.
Weirich, F.H., 1985. Sediment budget for a high energy glacial lake. Geografiska Annaler 67A, 83–99.
Woo, M.-K., 1986. Permafrost hydrology in North America. Atmosphere—Ocean 24, 201–234.
Zemp, M., Hoelzle, M., Haeberli, W., 2007. Distributed modelling of the regional climatic equilibrium line altitude of glaciers in the European Alps. Global and Planetary Change 56, 83–100.